

# Spectral Tuning in the Eyes of Deep-Sea Lanternfishes (Myctophidae): A Novel Sexually Dimorphic Intra-Ocular Filter

Fanny de Busserolles<sup>a, d, e</sup> Nathan S. Hart<sup>a</sup> David M. Hunt<sup>a, b</sup> Wayne I. Davies<sup>a</sup>  
N. Justin Marshall<sup>d</sup> Michael W. Clarke<sup>c</sup> Dorothee Hahne<sup>c</sup> Shaun P. Collin<sup>a, b</sup>

<sup>a</sup>School of Animal Biology and the Oceans Institute, <sup>b</sup>Lions Eye Institute, and <sup>c</sup>UWA Centre for Metabolomics, Metabolomics Australia, The University of Western Australia, Perth, W.A., and <sup>d</sup>Sensory Neurobiology Group, Queensland Brain Institute, University of Queensland, Brisbane, Qld., Australia; <sup>e</sup>Red Sea Research Centre, King Abdullah University of Science and Technology, Thuwal, Saudi Arabia

## Key Words

Yellow pigment · Retinal filter · Spectral tuning · Myctophids · Opsins · Microspectrophotometry · Bioluminescence · Sexual dimorphism

## Abstract

Deep-sea fishes possess several adaptations to facilitate vision where light detection is pushed to its limit. Lanternfishes (Myctophidae), one of the world's most abundant groups of mesopelagic fishes, possess a novel and unique visual specialisation, a sexually dimorphic photostable yellow pigmentation, constituting the first record of a visual sexual dimorphism in any non-primate vertebrate. The topographic distribution of the yellow pigmentation across the retina is species specific, varying in location, shape and size. Spectrophotometric analyses reveal that this new retinal specialisation differs between species in terms of composition and acts as a filter, absorbing maximally between 356 and 443 nm. Microspectrophotometry and molecular analyses indicate that the species containing this pigmentation also possess at least 2 spectrally distinct rod visual pigments as a result of a duplication of the *Rh1* opsin gene. After modelling the effect of the yellow pigmentation on photoreceptor spectral sensitivity, we suggest that this unique specialisa-

tion acts as a filter to enhance contrast, thereby improving the detection of bioluminescent emissions and possibly fluorescence in the extreme environment of the deep sea. The fact that this yellow pigmentation is species specific, sexually dimorphic and isolated within specific parts of the retina indicates an evolutionary pressure to visualise prey/predators/mates in a particular part of each species' visual field.

© 2015 S. Karger AG, Basel

## Introduction

The evolution of visual sensitivity appears to be driven primarily by the spectral range and intensity of available light within a species' visual environment. As a result, different visual pigments are found in the retina of different species, with spectral sensitivities broadly matching the surrounding light conditions [Lythgoe and Partridge, 1989]. Spectral adaptation to the photic environment is mainly achieved by two types of tuning mechanisms: variation in the number of spectral classes of photoreceptors through the loss or duplication of opsin genes, and variation in the type of chromophore within the photoreceptor outer segment [see Bowmaker and Hunt, 2006; Bowmaker, 2008; Davies et al., 2012, for review].

Due to the physical properties of water, aquatic animals can be found in a wide range of spectral environments, from clear blue oceanic water to turbid brown river water, and as a result possess different subsets of cone classes ranging from the presence of at least 1 representative of each of the 4 cone classes (Australian lungfish [Bailes et al., 2007]) at one extreme to the retention of just a single cone class (several species of sharks [Hart et al., 2011]) at the other, although it is not uncommon amongst deep-sea fishes to find that all 4 cone classes have been lost to leave a rod-only retina [Hunt et al., 2001]. In the open ocean, light conditions vary greatly with depth, decreasing in intensity and spectral range as the short and long wavelengths are attenuated. In the deep sea, only very low intensities of sunlight in the blue-green range remain below 200 m, creating a relatively dark environment accompanied by a multitude of bioluminescent emissions that are also mainly concentrated in the blue-green part of the visible light spectrum [Widder, 2002, 2010].

The eyes of deep-sea teleost fishes represent a good example of visual adaptation in spectral sensitivity. Most species have adapted to their dim-light environment by losing their cone photoreceptors (photopic vision) in favour of a single type of rod photoreceptor (scotopic vision) containing a single visual pigment encoded by the *Rh1* rod opsin gene. While most terrestrial and shallow water vertebrates usually have an *Rh1* visual pigment maximally absorbing around 500 nm, many deep-sea teleosts have shifted the spectral sensitivity of their rod pigment towards shorter wavelengths to spectrally match their ambient photic environment, i.e. maximal absorbance around 480 nm [Crescitelli, 1990; Douglas and Partridge, 1997; Douglas et al., 2003]. The tuning mechanism responsible for the spectral shift toward shorter wavelengths in the *Rh1* gene has been identified at the molecular level and occurs as a result of different combinations of substitutions at 8 different amino acid sites depending on the species [Hunt et al., 2001].

Like most mesopelagic fishes, lanternfishes (Myctophidae) possess several visual adaptations for life in the mesopelagic zone that serve to increase the sensitivity of the eye and optimise photon capture [de Busserolles et al., 2013, 2014a, b]. Lanternfishes generally lack cones and possess a single rod photoreceptor class with a peak spectral absorption tuned to the blue-green region of the visible spectrum [Partridge et al., 1992; Douglas and Partridge, 1997; Turner et al., 2009]. However, the presence of 2 photoreceptor classes has been found in a few species [Hasegawa et al., 2008; Turner et al., 2009]. In this study, we describe a novel visual adaptation, a retinal yellow pig-

mentation associated with a rod gene duplication, that is unique among vertebrates and assists lanternfishes to tune their visual sensitivity.

## Material and Methods

### Samples

Samples were collected in the Coral Sea during 3 cruises on the RV *Cape Ferguson* (AIMS, Townsville, Australia) in Autumn-Winter 2010–2012 under the following collection permits: Coral Sea waters (CSCZ-SR-20091001-01), Commonwealth waters (AU-COM2009051), GBRMPA (G09/32237.1) and Queensland Fisheries (133805) (Marshall, AEC #SNG/080/09/ARC), and in the Peru-Chile trench on the FS *Sonne* (Germany) in September 2010 (sampling permits obtained by the Chief Scientist, University of Tübingen, Germany). Sampling was performed at the surface (<5 m) during the night using an Isaacs-Kid Midwater Trawl fitted with buoys or a neuston net. For each individual, the standard length and rostral-caudal eye diameter were measured with digital callipers (to a precision of 0.1 mm) prior to dissection and fixation (table 1). Following the guidelines of the NH&MRC Australian Code of Practice, under our University of Western Australia Animal Ethic Protocol (RA/3/100/917), eyes were then enucleated, the cornea and lens were dissected free from the eye cup and tissue was fixed specifically for different analyses (4% paraformaldehyde, RNALater, 100% alcohol, liquid nitrogen). One individual of *Myctophum brachygnathum*, sampled in Hawaii in May 2011 and fixed in 5% formalin, was provided by the American Museum of Natural History, New York, N.Y., USA (table 1).

### Retinal Wholemounts and Spectrophotometry

For each species, eyes preserved in 4% paraformaldehyde in 0.1 M sodium phosphate buffer (pH 7.4, PFA) were dissected to reveal the location and shape of the yellow-pigmented patches of retinal tissue. Retinal wholemounts were made according to standard protocols [Stone, 1981; Coimbra et al., 2006, Ullmann et al., 2011] and mounted photoreceptor side up in 0.1 M phosphate buffer (pH 7.4) between two No. 1 glass coverslips. For one specimen of *Symbiolophorus rufinus*, the eye was dissected on board ship directly after capture and the retina wholemounted fresh in between two No. 1 coverslips and kept at  $-20^{\circ}\text{C}$  in a light-tight container until analysis.

The transmission of light (300–800 nm) through each retina was measured systematically every 0.5 or 1 mm (depending of the size of the retina) across the wholemount using spectrophotometry. Each transmission spectrum was ultimately converted to a corrected absorbance spectra at the wavelength of maximum absorbance of the yellow pigment ( $\lambda_{\text{YPmax}}$ ). The detailed methods used to carry out the spectrophotometry analyses are provided in the supplementary material (for all online suppl. material, see [www.karger.com/doi/10.1159/000371652](http://www.karger.com/doi/10.1159/000371652)). The  $\lambda_{\text{YPmax}}$  values were then mapped onto an outline of the retinal wholemount traced from the calibrated digital image in Adobe Illustrator CS4. The whole file was saved as a scalable vector graphics (.svg) file and imported into R v.2.15.0 (R Foundation for Statistical Computing, 2012) to construct the maps using custom scripts [Garza Gisholt et al., 2014]. For this study, the Gaussian kernel smoother from the Spatstat package was used to construct the iso-density maps [Baddeley and Turner, 2005]. For each map, the sigma value was adjusted to 30.

**Table 1.** Summary of the individuals analysed in this study that presented a yellow patch of retinal tissue

| Species                  | Sex | SL, mm | Eye $\phi$ , mm | Sampling location | Patches, n | Patch location |
|--------------------------|-----|--------|-----------------|-------------------|------------|----------------|
| <i>M. brachygnathum</i>  | F   | 65.7   | 6.8             | Coral Sea         | 1          | C              |
|                          | F   | 67.7   | 7.2             | Coral Sea         | 1          | C              |
|                          | F   | 69.7   | 7.5             | Coral Sea         | 1          | C              |
|                          | M   | 66.6   | 7.3             | Coral Sea         | 1          | T/V            |
|                          | M   | 67.7   | 7.5             | Coral Sea         | 1          | T/V            |
|                          | M   | 58.1   | 7.3             | Hawaii            | 1          | T/V            |
| <i>M. nitidulum</i>      | F   | 85.4   | 7.1             | Peru-Chile Trench | 1          | T/C            |
|                          | F   | 80.0   | 6.9             | Peru-Chile Trench | 1          | T/C            |
|                          | M   | 77.9   | 6.9             | Peru-Chile Trench | 1          | N              |
| <i>M. obtusirostre</i>   | M   | 92.4   | 10.6            | Coral Sea         | 1          | V              |
|                          | M   | 90.9   | 10.6            | Coral Sea         | 1          | V              |
| <i>M. lychnobium</i>     | F   | 106.1  | 11.1            | Coral Sea         | 2          | D + C/V        |
|                          | F   | 83.3   | 9.4             | Coral Sea         | 2          | D + C/V        |
| <i>M. spinosum</i>       | F   | 87.5   | 8.7             | Coral Sea         | 2          | D + C/V        |
| <i>M. aurolaternatum</i> | J   | 57.8   | 5.3             | Coral Sea         | 1          | V              |
| <i>S. rufinus</i>        | J   | 73.7   | 6.6             | Coral Sea         | 1          | D              |
|                          | J   | 62.5   | 6.1             | Coral Sea         | 1          | D              |
|                          | J   | 31.6   | 2.8             | Coral Sea         | 1          | D              |
| <i>S. evermanni</i>      | J   | 65.8   | 6.7             | Coral Sea         | 1          | D              |
|                          | J   | 53.8   | 4.8             | Coral Sea         | 1          | D              |
|                          | J   | 48.1   | 4.5             | Coral Sea         | 1          | D              |
| <i>G. tenuiculus</i>     | M   | 49.4   | 3.5             | Peru-Chile Trench | 2          | D + V          |
|                          | ?   | 43.1   | 2.9             | Peru-Chile Trench | 2          | D + V          |
|                          | ?   | 40.6   | 2.7             | Peru-Chile Trench | 2          | D + V          |
| <i>H. proximum</i>       | J   | 43.3   | 5.2             | Coral Sea         | 1          | D              |

For each individual, the sex (F = female, M = male, J = juvenile, ? = unknown), standard length (SL), eye diameter ( $\phi$ ), location of sampling and number of retinal yellow pigmented patches and their location (C = central, D = dorsal, T = temporal, N = nasal, V = ventral) are given.

### Cryosections

The retina of one individual of *Gonichthys tenuiculus*, preserved in 4% PFA, was processed for cryosectioning in order to visualise the position of the yellow pigmentation within the retina. Sections (40  $\mu$ m in thickness) were cut using a Leica CM1900 cryostat-microtome and mounted in VectaMount Aqueous medium (Vector Laboratories, USA). The sections were observed under an Olympus BX50 compound light microscope and pictures were taken with an Olympus DP70 digital camera.

### Identification of the Yellow Pigmentation

Yellow pigments have previously been observed in the eyes of vertebrates, either as a diffuse pigment within the lens and cornea or within the inner segment of the photoreceptors, i.e. in oil droplets or ellipsoids [Muntz, 1976; Appleby and Muntz, 1979; Goldsmith et al., 1984; Collin et al., 2003; Siebeck et al., 2003; Bailes et al., 2006]. These pigments have been identified as tryptophan de-

rivatives [van Heyningen, 1971a, b; Thorpe et al., 1992] or mycosporine-like amino acids [Thorpe et al., 1993] in the lens, and as carotenoids [Goldsmith et al., 1984] in the retina. Extraction methods for the yellow pigment found in the retina of the lanternfishes followed therefore the classic extraction protocols for these various group of compounds, using appropriate standards. Retinae of *M. aurolaternatum* and *Hygophum proximum* were dissected while on board ship, deep-frozen in liquid nitrogen in small Eppendorf tubes and stored at  $-20^{\circ}\text{C}$ . In order to extract any water-soluble pigments (e.g. tryptophan derivatives and other amino acids), the retina of *M. aurolaternatum* was thawed at room temperature and homogenised several times in a glass tube with 1 ml of distilled water (3 min at 30 Hz) [Truscott et al., 1992; Thorpe et al., 1993]. Extraction of possible carotenoids was performed as described by Toomey and McGraw [2007, 2009]. The retina of *H. proximum* was thawed and 10  $\mu$ l of *trans*- $\beta$ -apo-8-carotenal (1 ng/ $\mu$ l; Sigma Aldrich) and 50  $\mu$ l of retinyl acetate (1 ng/ $\mu$ l; Sigma Aldrich) were

added to the sample as internal standards. The sample was then homogenized in 1 ml of methanol for 3 min at 30 Hz and centrifuged (3 min at 13,000 rpm), and the supernatant was transferred into a glass tube. The procedure was repeated twice with 1 ml of 1:1 hexane:*tert*-butyl methyl ether (MTBE) and the supernatants combined. Since the yellow pigment was still present in the tissue and not in the supernatant, we repeated the procedure twice more with 1 ml of dimethyl sulfoxide (DMSO) [Sedmak et al., 1990].

#### Microspectrophotometry

The eyes of 3 species of lanternfishes, i.e. *M. obtusirostre*, *M. spinosum* and *S. evermanni*, were preserved for microspectrophotometry (MSP) according to Hart et al. [2011]. Specimens were collected alive and were dark adapted for 15 min before being euthanized following the guidelines of the NH&MRC Australian Code of Practice, under the University of Western Australia Animal Ethics Protocol (RA/3/100/917). Eyes were removed in the dark under dim red light, the cornea was removed and the whole eye was lightly fixed for 30 s in 2.5% glutaraldehyde in phosphate-buffered saline (PBS, 340 mosm · kg<sup>-1</sup>, pH 7.0), washed in PBS for 30 s and stored in PBS at 4 °C in a light-tight container until they were analysed back in the laboratory 3–4 weeks later.

In all cases, small pieces (~1 × 1 mm to 3 × 3 mm) of retina were mounted between No. 1 glass coverslips in a drop of 425 mosm · kg<sup>-1</sup> PBS containing 10% dextran (MW 282,000; Sigma D-7265). Absorbance spectra (330–800 nm) were made using a computer-controlled single-beam wavelength-scanning microspectrophotometer [Hart et al., 2004, 2011, 2012]. Due to the very small diameter of the rod photoreceptors of the lanternfish species analysed (<1 µm [de Busserolles et al., 2014b]), longitudinal ‘end-on’ absorbance spectra were measured from patches of rod outer segments. A sample scan was made by aligning the measuring beam (typical dimensions 10 × 10 µm) within a patch of rods in a specific part of the retina and recording the amount of light transmitted at each wavelength across the spectrum. Baseline scans were made in an identical way to sample scans but from a cell-free area of the preparation. The transmittance (ratio of sample to baseline signal) of the outer segments was calculated at each wavelength and converted to absorbance to give a pre-bleach spectrum. Each patch of rods was then bleached with broadband white light for 2 min and subsequent sample and baseline scans were made to create a post-bleach absorbance spectrum. Because we were measuring the absorbance through a patch of retina that contains other absorbing material (i.e. other retinal layers, yellow pigment) and not through a single rod outer segment, a difference spectrum was calculated by subtracting the post-bleach scan from the pre-bleach scan. Only spectra that satisfied established selection criteria [Levine and MacNichol Jr, 1985; Hart et al., 1998] were retained for further analysis. Difference absorbance spectra were analysed as described elsewhere [MacNichol Jr, 1986; Govardovskii et al., 2000; Hart, 2002] to provide an estimate of the wavelength of maximum absorbance ( $\lambda_{\max}$ ) of the retinal pigment contained in the rods, assuming that only one type of rod was present within the patch analysed. The mean  $\lambda_{\max}$  of a given pigment was then calculated from these individual patch  $\lambda_{\max}$  values. For display purposes, a mean difference absorbance spectrum was calculated by averaging the acceptable individual absorbance spectra.

To investigate the possibility that the photoreceptors of some species contained a mixture of visual pigment molecules utilizing both the A<sub>1</sub> and the A<sub>2</sub> chromophores, mean pre-bleach absor-

bance spectra (smoothed with a variable point unweighted running average) were fitted iteratively using the Excel Solver function in a custom macro written by N.S.H. with mixed-chromophore pigment templates to find the combination of visual pigment  $\lambda_{\max}$  (pure A<sub>1</sub>) and A<sub>1</sub>/A<sub>2</sub> ratio that gave the smallest sums of squares deviation between the real and modelled spectra between 0.8 and 0.2 normalised absorbance on the long-wavelength limb of the real spectrum (approximately the same region used to estimate  $\lambda_{\max}$ ) [Temple et al., 2010]. We made the assumption that only a single type of visual pigment opsin protein was expressed in each rod within the patch of rods and used established A<sub>1</sub> and A<sub>2</sub> visual pigment templates [Govardovskii et al., 2000] and a known relationship between the  $\lambda_{\max}$  values of A<sub>1</sub> and A<sub>2</sub> visual pigment pairs [Parry and Bowmaker, 2000].

#### Molecular Analyses

Eye and muscle tissues from *S. evermanni* were preserved for molecular analyses by immersion in RNALater and 100% alcohol, respectively, followed by storage at –20 °C. Genomic DNA (gDNA) was extracted from the muscle tissue using a DNeasy Blood and Tissue Kit (Qiagen) following the protocol provided by the manufacturer. First-round PCR amplifications utilized the ‘All-Opsins, All-Species’ (AOAS) degenerate PCR primer set F1/R2 designed by Davies et al. [2009]. A second hemi-nested PCR was carried out with primer sets F1/R1 and F2/R2 [Davies et al., 2009]. The sequences of the primers used in this study along with the annealing temperatures used and expected PCR products are provided in online supplementary table S1.

RNA was extracted from eye tissue using a PureLink RNA Mini Kit (Invitrogen) and cDNA synthesized using a 5′/3′ RACE Kit, 2nd generation (Roche), according to the manufacturer’s instructions. Opsin sequences were amplified from cDNA using primer sets designed to amplify vertebrate opsins. The resulting amplified fragments were sequenced and the sequences used to design primers for RACE in order to extend the sequences at the 3′ ends.

All PCR amplifications were performed using a HotStarTaq DNA Polymerase Kit (Qiagen). Following a heat activation step of 15 min at 95 °C, 45 cycles were performed with a denaturation step of 30 s at 94 °C, an annealing step of 60 s at 45–50 °C, an extension step of 90 s at 72 °C and a final extension of 10 min at 72 °C. Gel-purified (Wizard SV Gel and PCR Clean-Up System; Promega) PCR products were sequenced via the Sanger method.

Phylogenetic trees, including the *S. evermanni* opsin genes sequenced in this study, were constructed by neighbour joining [Saitou and Nei, 1987] and maximum likelihood using nucleotide sequences. All sequences were aligned in Clustal Omega [Sievers et al., 2011] and refined by eye. The parameters for the phylogenetic analysis, carried out using the MEGA phylogenetic package [Tamura et al., 2013], were pair-wise deletion and Kimura 2-parameter correction. The degree of support for internal branching was assessed by bootstrapping with 1,000 replicates.

#### Modelling of the Association of the Yellow Pigment and the Visual Pigments

The effect of the yellow pigmentation on the spectral sensitivity of the rods was modelled for 2 species: *M. obtusirostre* and *S. evermanni*. For each species, the quantal spectral sensitivity of the rod photoreceptors associated with the yellow pigmentation was modelled by multiplying the species-specific axial spectral absorbance of the rod outer segment by the spectral transmittance of the

species-specific overlying yellow pigmentation. We used visual pigment templates [Govardovskii et al., 2000] of appropriate  $\lambda_{\max}$  for the modelling. Normalised absorbance templates were converted to axial outer segment absorbance by assuming a visual pigment specific (decadic) absorbance of  $0.013 \mu\text{m}^{-1}$  (rhodopsin [Turner et al., 2009]) and a rod outer segment length of  $39 \mu\text{m}$  for *S. evermanni* [de Busserolles et al., 2014b] and  $45 \mu\text{m}$  for *M. obtusirostre* as per a similar species (*M. brachygnathum* [de Busserolles et al., 2014b]). Measurements of ocular media transmittance could not be made from fresh specimens at sea and so were excluded from the modelling.

## Results

### Description of the Yellow Pigment

Yellow pigmentation within the retina was noted in 10 species of lanternfishes from 4 different genera all belonging to a single subfamily, i.e. the Myctophinae (table 1). After detailed observation of 6 species, the distribution of the yellow pigmentation appeared to be species specific, varying in location, shape, size and number of patches (fig. 1a–f). Maps of the corrected absorbance at  $\lambda_{\text{YPmax}}$  for each species correlated very well with the visual observations and indicated that the pigmentation was restricted to well-defined retinal regions (fig. 1g–l). The maximum corrected absorbance at  $\lambda_{\text{YPmax}}$  varied between species from 0.78 (*S. evermanni*, fig. 1j) to 2.02 (*G. tenuiculus*, fig. 1g). Two of the 6 species analysed showed 2 patches of yellow pigmentation; *G. tenuiculus* possesses 2 ovoid-like patches, i.e. a small one in the dorsal part of the retina and a larger one in the ventral retina (fig. 1a), whereas *M. lychnobium* possesses extensive pigment patches covering the entire dorsal part of the retina and the centro-ventral retina arranged in a streak-like pattern (fig. 1e). The 4 other species all possess a single patch of yellow pigmentation. *H. proximum*, *S. rufinus* and *S. evermanni* all have an ovoid-shaped patch situated in the dorsal or dorso-nasal part of the retina (fig. 1b–d, respectively), whereas *M. obtusirostre* possesses a streak-like patch in the temporo-ventral area (fig. 1f). The density of the yellow pigmentation appears to vary between species, with some showing very intense yellow pigmentation (i.e. *G. tenuiculus*, *H. proximum*, *S. rufinus* and *S. evermanni*, fig. 1a–d) and others paler pigmentation (i.e. *M. lychnobium* and *M. obtusirostre*, fig. 1e, f).

Sections through the retina of *G. tenuiculus* reveal that the yellow pigmentation is situated within the outer nuclear layer (fig. 2). The pigmentation appears to be evenly distributed and does not appear to be compartmentalised within any organelles (i.e. oil droplets and ellipsosomes).

### Sexual Dimorphism

A sexual dimorphism in the size, shape and location of the yellow pigmentation was observed in 2 species, i.e. *M. brachygnathum* and *M. nitidulum*, out of the 10 analysed (fig. 3). In *M. brachygnathum* (fig. 3a), this sexual dimorphism was observed in all 3 females and all 3 males examined. The females possess a small yellow patch in the central part of the retina just ventral to the optic nerve head. The males possess a larger yellow patch at the periphery of the temporo-ventral retina. In *M. nitidulum* (fig. 3b), there also appears to be a sexual dimorphism although this will have to be confirmed as only 2 females and 1 male were examined. In the females, the yellow patch takes the shape of a band extending from the temporal to the ventral retina, located ventral to the optic nerve head. In the male, the patch is approximately circular and located in the nasal periphery. At this stage, it is unknown whether the other 8 species with retinal yellow pigmentation also have a sexual dimorphism as either both sexes were not collected or only immature specimens were available (table 1).

### Spectrophotometry and Pigment Extraction

Spectrophotometric analysis of the unfixed frozen retinal wholemount of *S. rufinus* revealed that the chemical fixation process had little effect on the absorbance of the yellow pigmentation, with a difference in  $\lambda_{\text{YPmax}}$  between the fresh and fixed samples of only 3 nm and a difference in full width at half maximum (FWHM) of 12 nm (online suppl. fig. S1).

Spectrophotometric analysis of the retinal wholemounts of different species revealed that the yellow pigmentation acts as a short-wavelength-absorbing (long-pass) filter (fig. 4). The maximum absorbance of the yellow pigmentation ( $\lambda_{\text{YPmax}}$ ) varies from 356 nm (*M. obtusirostre*, fig. 4f) to 443 nm (*G. tenuiculus*, fig. 4a). Comparison of the spectral curves, based on the  $\lambda_{\text{YPmax}}$  from the different species (fig. 4), suggests that at least 3 different types of yellow pigments/filters are present with a peak absorbance at approximately 350, 380 and 440 nm. In addition, some of these pigments may be present as mixtures. This might be the case for *H. proximum* (fig. 4b), which seems to possess a mixture of the pigment present in *M. obtusirostre* (fig. 4f), *G. tenuiculus* (fig. 4a) and *M. lychnobium* (fig. 4e).

In order to identify the nature of the yellow pigmentation, extraction was attempted from the retinas of 2 species, i.e. *M. aurolaternatum* and *H. proximum*, using water in the former species to extract water-soluble compounds and organic solvents in the latter species to extract carotenoids. However, in each case, the yellow pigment

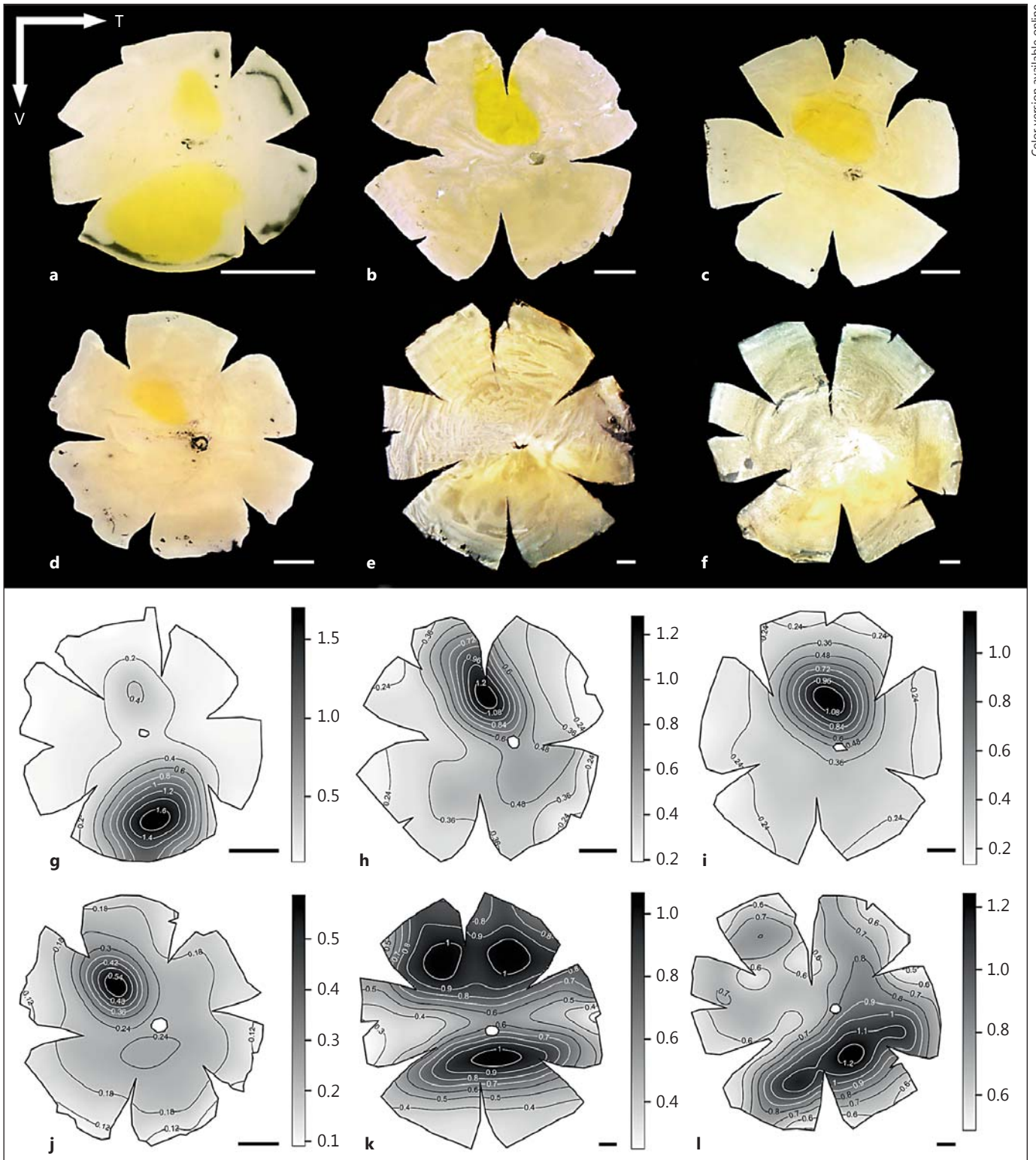


**Fig. 1.** Diversity in the yellow pigmentation distribution across the retina of 6 species of lanternfishes. **a–f** Retinal wholemount visual observations. **g–l** Maps of corrected absorbance at the wavelength of peak absorbance of the yellow pigmentation  $\lambda_{YP,max}$ . *G. tenuiculus* (**a, g**), *H. proximum* (**b, h**), *S. rufinus* (**c, i**), *S. evermanni* (**d, j**), *M. lychnobium* (**e, k**) and *M. obtusirostre* (**f, l**). The arrows indicate the orientation of the retinal wholemount (T = temporal, V = ventral). Scale bars = 1 mm. Colour refers to the online version only.

*lus* (**a, g**), *H. proximum* (**b, h**), *S. rufinus* (**c, i**), *S. evermanni* (**d, j**), *M. lychnobium* (**e, k**) and *M. obtusirostre* (**f, l**). The arrows indicate the orientation of the retinal wholemount (T = temporal, V = ventral). Scale bars = 1 mm. Colour refers to the online version only.

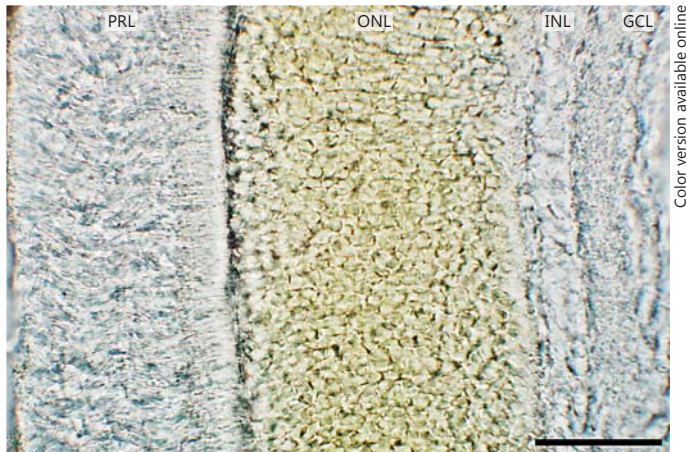


**Fig. 2.** Location and distribution of the yellow pigmentation in the retina of *G. tenuiculus*. PRL = Photoreceptor layer; ONL = outer nuclear layer; INL = inner nuclear layer; GCL = ganglion cell layer. Scalebar = 50  $\mu\text{m}$ . Colour refers to the online version only.

proved to be refractory to extraction, thereby eliminating amino acids, tryptophan derivatives, lipophilic/hydrophilic pigments and carotenoids as the main constituents in the species analysed.

#### Microspectrophotometry

Microspectrophotometric results for the 3 species analysed are summarized in table 2. The mean difference spectra for each type of rod in each species are shown in figure 5. Except for *M. spinosum*, in which only a single spectral class of rod photoreceptor was identified (492 nm, fig. 5c), several spectral classes of rod photoreceptors were found in the other 2 species.

For *M. obtusirostre*, 2 classes of rod photoreceptors were identified with mean  $\lambda_{\text{max}}$  values of 473 nm in the non-yellow retinal area and 527 nm in the area containing the yellow pigmentation (fig. 5b). On the basis of goodness of fit to established  $A_1$  and  $A_2$  visual pigment templates [Govardovskii et al., 2000], the pigment in the 473-nm rod was considered to represent 100%  $A_1$  and the pigment in the 527-nm rod was considered to represent 100%  $A_2$ . However, given the known relationship between the  $\lambda_{\text{max}}$  values of  $A_1$  and  $A_2$  visual pigment pairs [Parry and Bowmaker, 2000], it is very likely that these two pigments originate from two different opsins, since replacement of an  $A_1$  by an  $A_2$  chromophore would only shift the  $\lambda_{\text{max}}$  of the 473-nm pigment to 484 nm.

For *S. severmanni*, 3 classes of rod photoreceptor were identified with mean  $\lambda_{\text{max}}$  values of 476, 503 and 512 nm

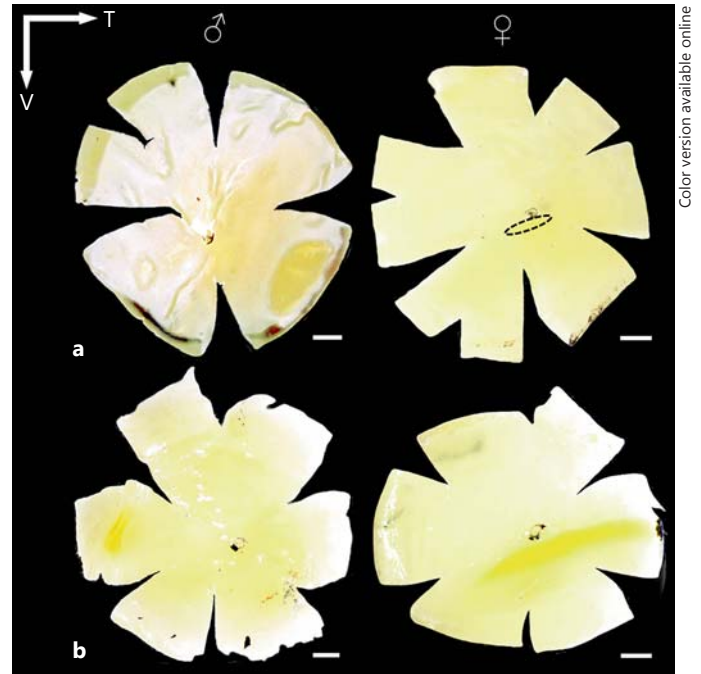


**Fig. 3.** Retinal wholemounts showing the sexual dimorphism in the yellow pigment in two species of lanternfish, i.e. *M. brachygnathum* (a) and *M. nitidulum* (b). The yellow patch in the female *M. brachygnathum* is highlighted by a dotted line. The arrows indicate the orientation of the retinal wholemount (T = temporal, V = ventral). Scale bars = 1 mm. Colour refers to the online version only.

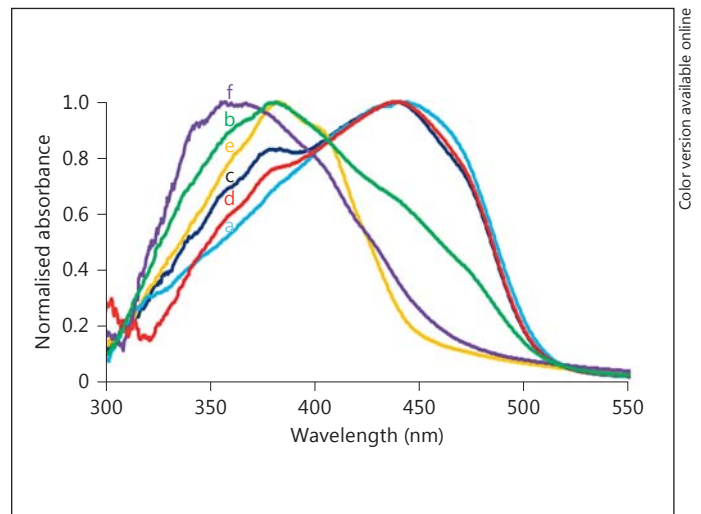


**Fig. 4.** Normalised corrected absorbance spectra of the yellow pigment in 6 lanternfish species, i.e. *G. tenuiculus*,  $\lambda_{\text{YPmax}} = 443$  nm (a), *H. proximum*,  $\lambda_{\text{YPmax}} = 381$  nm (b), *S. rufinus*,  $\lambda_{\text{YPmax}} = 438$  nm (c), *S. evermanni*,  $\lambda_{\text{YPmax}} = 439$  nm (d), *M. lychnobium*,  $\lambda_{\text{YPmax}} = 383$  nm (e) and *M. obtusirostre*,  $\lambda_{\text{YPmax}} = 356$  nm (f).

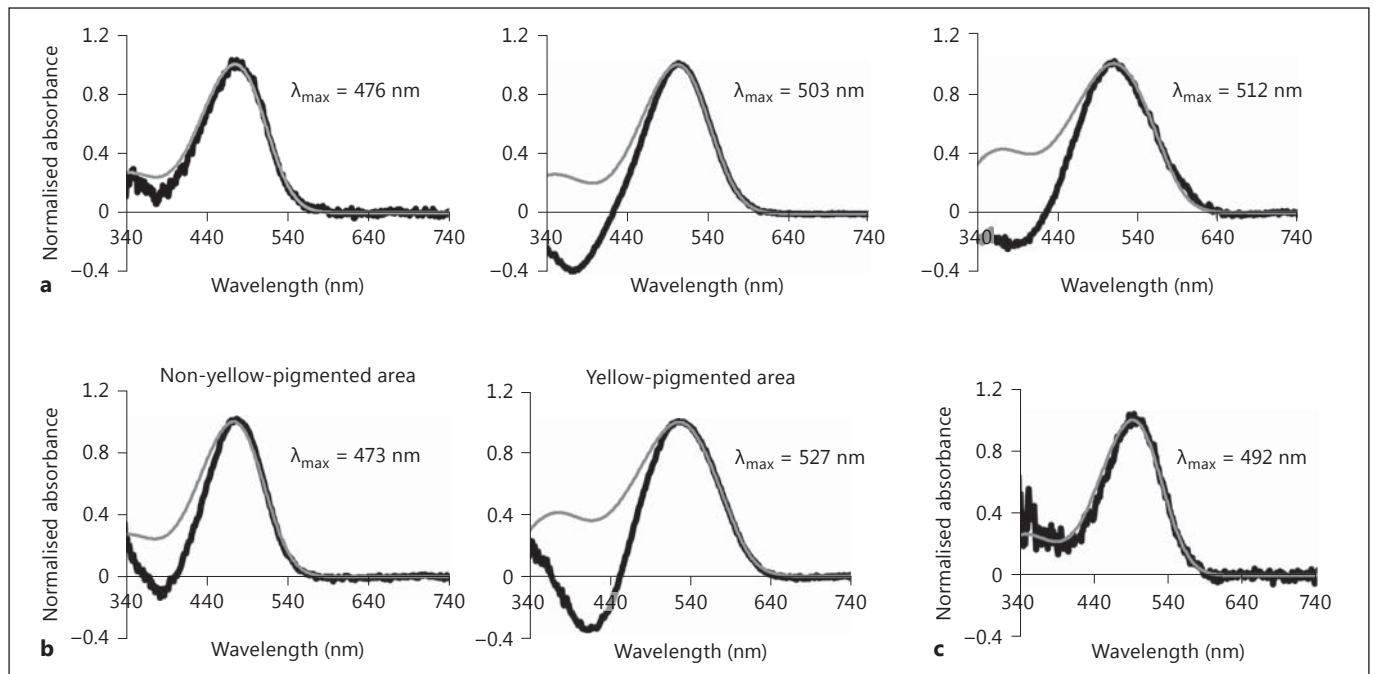


**Fig. 5.** Mean bleaching difference absorbance spectra of the rod visual pigments in 3 species of lanternfishes, i.e. *S. evermanni* (a), *M. obtusirostre* (b) and *M. spinosum* (c). The wavelength of maximum absorbance ( $\lambda_{\max}$ ) is also provided for each species. Spectra (black lines) are fitted with visual pigment templates (grey lines [Govardovskii et al., 2000]) of appropriate  $\lambda_{\max}$  value. For *M. obtusirostre* (b), the absorbance spectra were measured in non-yellow- and yellow-pigmented areas of retinal tissue.

**Table 2.** Spectral absorption characteristics of rod visual pigments in the retina of 3 myctophids species measured using MSP

|   | <i>M. spinosum</i> |  | <i>M. obtusirostre</i> |                 | <i>S. evermanni</i> |                 |                                |
|---|--------------------|--|------------------------|-----------------|---------------------|-----------------|--------------------------------|
|   | 1                  |  | 1                      | 2               | 1                   | 2               | 3                              |
| Scans analysed, n                             | 7                  |  | 4                      | 9               | 4                   | 10              | 6                              |
| Chromophore                                   | A <sub>1</sub>     |  | A <sub>1</sub>         | A <sub>2</sub>  | A <sub>1</sub>      | A <sub>1</sub>  | A <sub>1</sub> +A <sub>2</sub> |
| Mean $\lambda_{\max}$ ( $\pm 1$ SD), nm       | 492.1 $\pm$ 4.3    |  | 473.4 $\pm$ 1.7        | 527.3 $\pm$ 1.1 | 475.9 $\pm$ 1.2     | 503.4 $\pm$ 1.4 | 512.7 $\pm$ 7.4                |
| $\lambda_{\max}$ of the mean spectrum, nm     | 492.4              |  | 473.2                  | 526.5           | 476.0               | 503.5           | 511.9                          |
| Maximum corrected absorbance <sup>1</sup>     | 0.020              |  | 0.058                  | 0.055           | 0.023               | 0.126           | 0.062                          |
| Running average <sup>2</sup> $\lambda_{\max}$ | 494                |  | 477                    | 528             | 477                 | 505             | 510                            |

<sup>1</sup> Measured at the  $\lambda_{\max}$  of the bleaching difference spectrum. <sup>2</sup> Variable-point unweighted running average maximum of the data, which is a measure of the wavelength of peak absorbance of the pigment that is independent of any assumptions as to the type of chromophore (A<sub>1</sub> or A<sub>2</sub>) present.

(fig. 5c). While the 476- and 503-nm pigments were found to be best fitted by A<sub>1</sub>-based templates, the 512-nm pigment was best fitted by a template derived from a mixture of 47% A<sub>1</sub> and 53% A<sub>2</sub>. Although both the 476- and the 503-nm pigments possess 100% A<sub>1</sub> chromophore, thereby indicating the presence of 2 different opsins, it is un-

likely that the 512-nm pigment originates from a third opsin. Most probably, the 512-nm pigment contains the same opsin as the 503-nm pigment, with the difference in wavelength arising from the presence of both A<sub>1</sub> and A<sub>2</sub> chromophores within their outer segments.

### Molecular Analyses

Two opsin transcripts, identified as encoded by 2 *Rh1* opsin genes, were PCR-amplified from *S. evermanni* retinal cDNA. The sequences were aligned with the *Rh1* rod opsin and representatives of all 4 cone opsin coding sequences of the zebrafish *Danio rerio* using Clustal Omega [Sievers et al., 2011]. These alignments were then used to generate neighbour-joining and maximum-likelihood phylogenetic trees (online suppl. fig. S2). In both cases, both *S. evermanni* sequences fall into the same clade as the zebrafish *Rh1* sequences, thereby confirming that both are *Rh1* opsin orthologues. The two sequences were designated as *Rh1-A* and *Rh1-B*.

*Rh1-A* and *Rh1-B* differ at specific sites that have previously been shown to be important for spectral tuning [Hunt et al., 2001] (online suppl. fig. S3); *Rh1-B* possesses Tyr rather than Phe at site 261 and Ala rather than Ser at site 292. These two substitutions in *Rh1-B* would be expected to result in a long-wavelength shift in the absorbance peak of the pigment compared to *Rh1-A*, and extrapolation from pigments in other species with identical substitutions would indicate a red shift of around 20–25 nm [Yokoyama et al., 1995; Hunt et al., 1996]. This is consistent with the different  $\lambda_{\max}$  values found using MSP for rod photoreceptors in this species.

Despite several attempts to complete the sequence of *Rh1-A*, the 5' end remained truncated; the missing portion includes 2 potential tuning sites (sites 83 and 122). However, since *Rh1A* shows a spectral sensitivity similar to that of the other myctophid rod opsins (~470 nm), which possess Asp83 and Gln122 [Yokoyama et al., 2008], as does *Rh1-B* (the long-wave-shifted rod), it is unlikely that either of these sites in *Rh1-A* is substituted.

*Rh1-A* and *Rh1-B* nucleotide sequences from *S. evermanni* were aligned with all of the myctophid *Rh1* opsin sequences available in GenBank, plus the *Rh1* opsin gene nucleotide sequences of the short-fin pearleye *Scopelarchus analis*, the zebrafish *D. rerio*, the yellow river scaleless carp *Gymnocypris eckloni* and the elephant shark *Callorhynchus milii*. The *Rh2* opsin gene nucleotide sequence of *D. rerio* served as an out group. Neighbour-joining and maximum-likelihood analyses were carried out on the aligned nucleotide sequences and the resultant trees (fig. 6) both grouped the *S. evermanni* sequences with those from *Electrona antarctica* and the two *Benthosema* species. The precise location of the *S. evermanni* differed, however, between the two methods, with neighbour joining placing the *S. evermanni Rh1-B* sequences subsequent to the evolution of the *Benthosema* genus and the maximum-likelihood method placing the *S. evermanni Rh1-B*

sequence on a separate branch with the *B. pterotum* sequence only. The relevant bootstrap values are all relatively low, reflecting the overall similarity of the myctophid *Rh1* sequences. It would appear, therefore, that the *Rh1* duplication in *S. evermanni* arose within the clade defined by 3 genera, i.e. *Symbolophorus*, *Benthosema* and *Electrona*, but its precise location cannot be further verified.

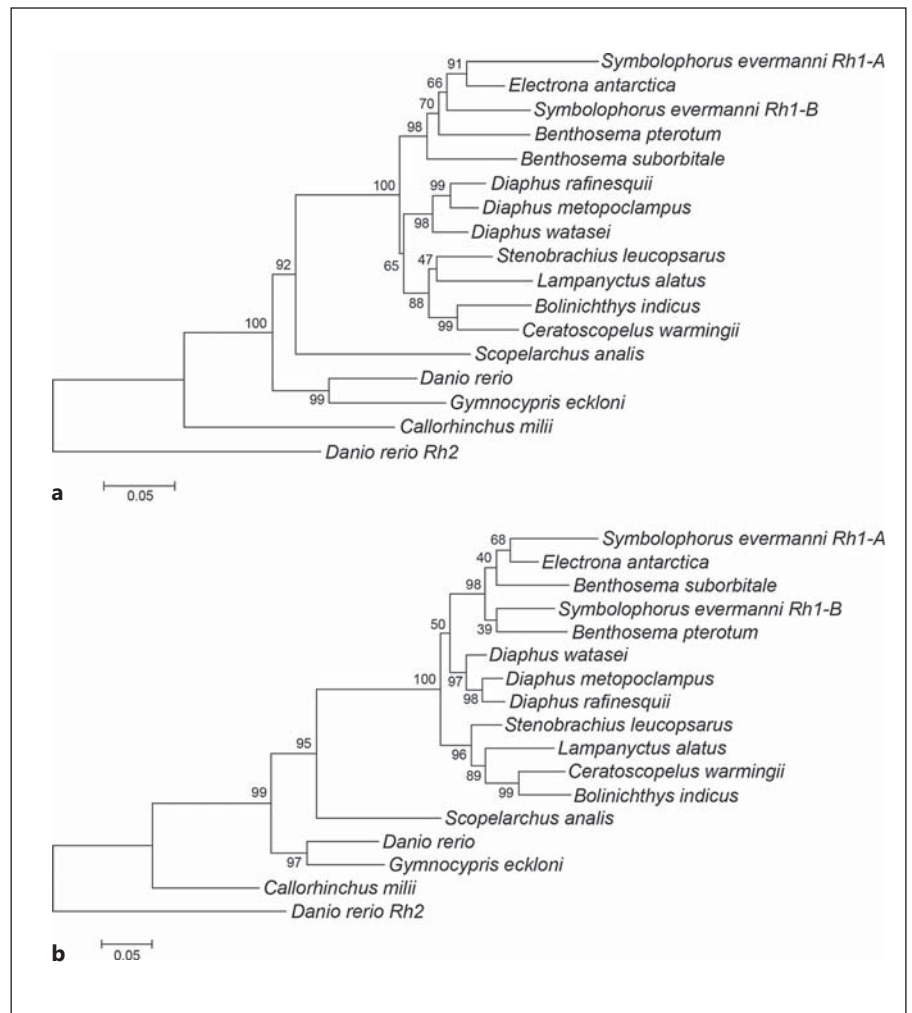
### Modelling of the Effects of the Yellow Pigment on Photoreceptor Spectral Sensitivity

Following our observations and measurements using MSP in yellow- and non-yellow-pigmented areas of the retina of *M. obtusirostre*, we concluded that the yellow pigmentation was only associated with the long-wave-shifted rod visual pigment and, as a result, only modelled this scenario in both species. Species-specific data were used to model the filtering effect of the yellow pigment on the photoreceptor spectral sensitivity (i.e. species-specific rod outer segment spectral absorbance and species-specific yellow pigment spectral transmittance).

Results show that the yellow filter decreases the absolute sensitivity at the peak of the long-wave-shifted rod visual pigment, shifts the overall sensitivity peak slightly toward longer wavelengths, and narrows the spectral sensitivity function by absorbing strongly at short wavelengths (fig. 7, 8). In *M. obtusirostre*, the yellow pigment narrows the FWHM bandwidth of the long-wave-shifted visual pigment from 248 nm to 142 nm (fig. 7) and shifts the peak of maximum absorbance of the rods 6 nm toward longer wavelengths.

In contrast to *M. obtusirostre*, 2 long-wave-shifted rod visual pigments were found in *S. evermanni* (fig. 8a). However, it is unknown if the yellow pigment is associated with both long-wave-shifted visual pigments or only one of the two. As a consequence, 3 different scenarios were modelled (fig. 8b–d). For the 503-nm visual pigment, the FWHM of the rods would decrease from 125 to 93 nm with the addition of the yellow pigment, while for the 512-nm visual pigment, the FWHM would decrease from 149 to 108 nm. In terms of the wavelength of maximum absorbance of the rod spectral sensitivity function, a slight shift toward longer wavelengths would be predicted with the addition of the yellow pigment (a 10-nm shift for rods containing the 503-nm pigment and an 8-nm shift for the 512-nm pigment). Depending on the scenario, *S. evermanni* could possess rods with peaks of quantal spectral sensitivity at 476, 513 and 520 nm if both of the long-wave-shifted visual pigments are associated

**Fig. 6.** Origin of the *Rh1* rod opsin gene duplication in *S. evermanni* within the Myctophidae. Phylogenetic trees were constructed via the neighbour-joining [Saitou and Nei, 1987] (a) and maximum likelihood (b) methods using *Rh1* opsin gene nucleotide sequences of *Diaphus metopoclampus* (JN544536), *D. rafinesquii* (JN412587), *D. watasei* (JN231003), *Stenobranchius leucopsarus* (EU407251), *Lampanyctus alatus* (JN412575), *C. warmingii* (JN412573), *Bolinichthys indicus* (JN412574), *Benthoema suborbitale* (JN412576), *B. pterotum* (JN231002), *E. antarctica* (AY141258), *S. analis* (EF517404), *D. rerio* (HM367063), *G. eckloni* (EU606010) and *C. milii* (EF565167). The *Rh2* opsin gene nucleotide sequence of *D. rerio* (NM131253) was added as a supplementary out group. The bootstrap confidence values are shown for each branch. The scale bar is calibrated at 0.05 substitutions per site.



with the yellow pigment (fig. 8b), or at 476, 513 and 512 nm (fig. 8c) or 476, 503 and 520 nm (fig. 8d) if only one or the other of the long-wave-shifted visual pigments is associated with the yellow pigment.

## Discussion

### *The Unique Yellow Pigment in the Retina of Myctophids*

In this study, we describe a novel visual specialisation, a photostable yellow pigmentation, present in the retina of several species of lanternfishes. Retinal photostable yellow pigmentation has previously been observed in a number of animals including species of lamprey [Collin et al., 2003] and lungfish [Bailes et al., 2006], the ornate dragon lizard [Barbour et al., 2002] and Amazonian cichlid fishes

[Muntz, 1973]. However, in contrast to these other animals, the yellow pigmentation in lanternfishes is restricted to well-defined areas (patches) of the retina, which appear to be species specific in terms of number, size, location and pigment density. Moreover, the location of the yellow pigmentation throughout the outer nuclear layer of the retina of myctophids differs from what has been previously observed in other species, where it is found within the distal region of the inner segment and/or diffusely distributed within the myoid region of the photoreceptors [Barbour et al., 2002; Collin et al., 2003; Bailes et al., 2006].

Unfortunately, the composition of the yellow pigmentation in myctophids could not be identified in this study. Colouration in animals is primarily due to the presence of melanins and carotenoids, although other types of pigment have been shown to be responsible for

**Fig. 7.** Modelling of the quantal spectral sensitivity of the two visual pigments measured in *M. obtusirostre*, without the presence of the yellow pigmentation (**a**) and with the yellow pigmentation associated with the long-wave-shifted visual pigment (527 nm) (**b**). Black line: 473 nm, grey line: 527 nm.

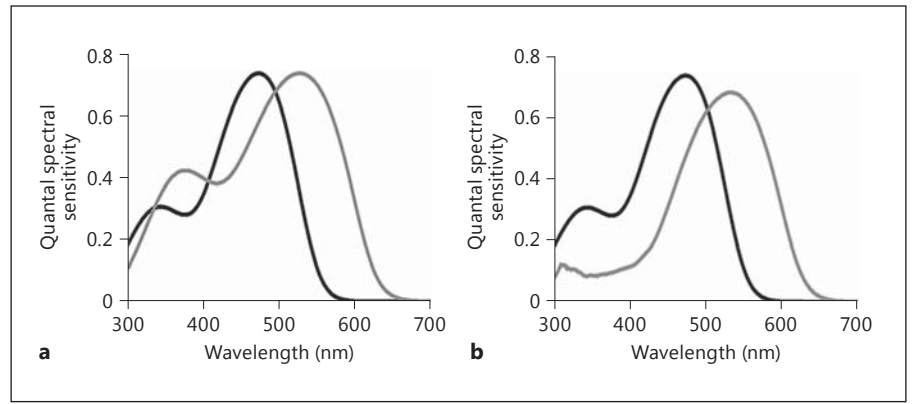
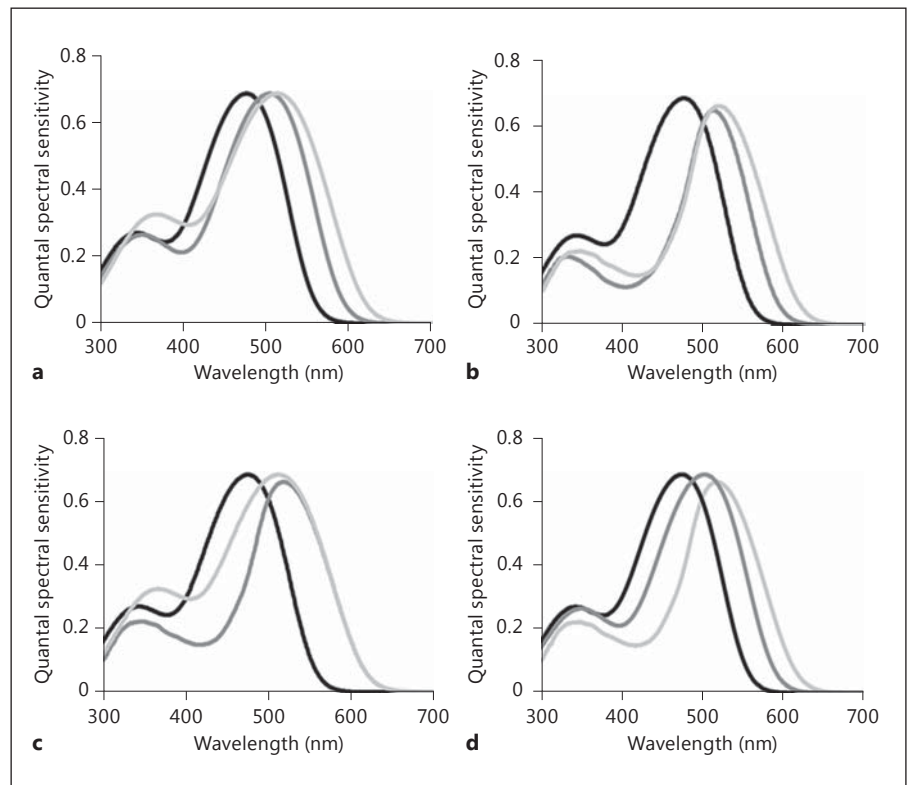


**Fig. 8.** Modelling of the effect of the yellow pigmentation on the quantal spectral sensitivity of rod photoreceptors in *S. evermanni*. Quantal spectral sensitivity of the three visual pigments (476 nm: black, 503 nm: dark grey, 512 nm: light grey) without the presence of the yellow pigmentation (**a**). Different scenarios where the yellow pigmentation is associated with the two long-wave-shifted visual pigments (**b**), the 503-nm visual pigment only (**c**) and the 512-nm visual pigment only (**d**).



animal colouration, i.e. porphyrins, pterins, flavins, psittacofulvins, [McGraw, 2006] and amino acids [Thorpe et al., 1993]. Specifically, yellow pigmentation in ocular tissues has been identified as carotenoids (in pufferfish cornea [Appleby and Muntz, 1979], in avian retinal oil droplets [Goldsmith et al., 1984] and in the human macula [Bone et al., 1985]), as tryptophan derivatives (in the lens of terrestrial vertebrates [van Heyningen, 1971a, b] and in the lenses of deep-sea fishes [Thorpe et al., 1992]) and as mycosporine-like amino acids (in the lenses of deep-sea fishes [Thorpe et al.,

1993]). Results from our study seem to exclude all of these compounds plus lipophilic or hydrophilic pigments (e.g. porphyrins and psittacofulvins) since water and non-polar solvents were also unsuccessful. However, extraction was only performed in 2 species: *M. auro-laternatum*, for which no spectrum is available, and *H. proximum*. Since no carotenoids were extracted in *H. proximum*, the pigment present in *H. proximum* and the two other species with similar spectra, i.e. *M. lych-nobium* and *M. obtusirostre*, may therefore not be carotenoid based, unless the bond occurs in a way that

does not allow extraction with standard methods. The spectra obtained for the pigment in the remaining three species, i.e. *G. tenuiculus*, *S. evermanni* and *S. rufinus*, are, however, different, with 2 peaks that are broadly similar to spectra obtained from carotenoids [Goldsmith et al., 1984]. So, although it would seem unlikely that the pigmentation has a different basis between species, this cannot be ruled out. Further analyses will have to be conducted to confirm the presence/absence of these compounds in all species and investigate other possibilities.

Melanins are often implicated in animal colouration and provide the black pigmentation of the retinal pigment epithelium. They exist, however, in two distinct forms, i.e. brown to black eumelanin and yellow to red pheomelanin. Melanin is also known to be difficult to extract from tissues due to its heterogeneous nature and its association with proteins [Taft, 1949; Liu et al., 2003]. Therefore, the difficulty in extracting the lanternfish yellow pigment could be consistent with the presence of a melanin and its colour would indicate that it is composed of pheomelanin. Although pheomelanin has yet to be directly observed in fishes [Ito and Wakamatsu, 2003], the presence of agouti signalling proteins (ASIP), which control the production of pheomelanin, in several fishes, i.e. goldfish [Cerdeira-Reverter et al., 2005], zebrafish and several species of pufferfishes [Klovins and Schiöth, 2005], indicates that it may be present; it could therefore be one of the components of the yellow pigmentation in lanternfishes.

Another unique feature of the yellow pigmentation in lanternfishes is its sexual dimorphism, observed so far in 2 species of the genus *Myctophum*. Although sexual dimorphism in the visual system has already been observed in insects (houseflies [Franceschini et al., 1981; Zeil, 1983], march flies [Hornstein et al., 2000], moths [Meyer-Rochow and Lau, 2008] and butterflies [Arikawa et al., 2005; Sison-Mangus et al., 2006]), crustaceans (copepods [Land, 1984, 1988]) and primates [Hunt et al., 2005], to our knowledge, this is the first observation of sexual dimorphism in the visual system of any non-primate vertebrate. Within these examples, sexual dimorphism in the visual system has been observed at several levels, i.e. eye morphology (flies [Franceschini et al., 1981; Zeil, 1983]), retinal organisation (flies [Zeil, 1983; Hornstein et al., 2000]), and spectral sensitivity (butterflies [Arikawa et al., 2005; Sison-Mangus et al., 2006] and primates [Hunt et al., 2005]). Lanternfishes show a new type of sexual dimorphism in the visual system, functionally similar to the visual sys-

tem of the small white butterfly *Pieris rapae crucivora* [Arikawa et al., 2005], where a filter is present in the ommatidia, which tunes visual sensitivity. However, in contrast to the small white butterfly, both male and female lanternfishes possess the filter but in different areas of the retina.

#### *Visual Pigments and Spectral Tuning in Myctophids*

The presence of different spectral classes of the rod photoreceptors in 2 lanternfish species with yellow retinal pigmentation indicate the presence of more than one visual pigment. While most lanternfish species possess a single photoreceptor class [Turner et al., 2009], 2 photoreceptor classes have been observed in 4 other species, i.e. *Ceratoscopelus warmingii* [Douglas et al., 2003], *H. proximum*, *M. aurolaternatum* [Turner et al., 2009] and *M. nitidulum* [Hasegawa et al., 2008], with the last 3 species all possessing yellow pigmentation (this study). Based on the conclusions of this study and known relationships between the  $\lambda_{\max}$  values of  $A_1$  and  $A_2$  visual pigment pairs [Parry and Bowmaker, 2000], the presence of two different opsins can be predicted for *H. proximum*, *M. nitidulum*, [Hasegawa et al., 2008; Turner et al., 2009], *M. obtusirostre* and *S. evermanni*. This was confirmed at the molecular level for *S. evermanni* (this study).

A pure rod retina with a single *Rh1* pigment is typical among deep-sea fishes [Hunt et al., 2001]. However, analysis of the rod opsin coding sequences expressed in *S. evermanni* revealed the presence of 2 *Rh1* opsin genes (*Rh1-A* and *Rh1-B*). This is only the second case of a rod opsin duplication recorded for a deep-sea fish, the first being the pearleye *S. analis* [Pointer et al., 2007]. However, in contrast to *S. analis*, for which the duplication of *Rh1* results in 2 spectrally similar visual pigments (486 and 479 nm [Pointer et al., 2007]), duplication in *S. evermanni* gives rise to 2 spectrally distinct visual pigments, with peaks at 476 and 503 nm. Moreover, while the 2 *Rh1* genes are phylogenetically different in *S. analis*, indicating an early duplication in evolutionary history [Pointer et al., 2007], the *Rh1-A* and *Rh1-B* genes in *S. evermanni* are phylogenetically very similar, indicating the origin of the duplication within a clade defined by 3 genera of myctophids. The fact that this duplication appeared at a specific stage in the evolutionary history of the family, and is only present in the Myctophinae subfamily, could explain why it has not been reported previously.

*Rh1* gene duplications have only been reported in teleost fishes and, even then, are quite rare. In addition to

the two deep-sea species mentioned above, it has been observed in the cyprinid zebrafish *D. rerio* [Morrow et al., 2011] and a few eel species [Hunt et al., 2013]. The expression of the second *Rh1* gene in the eel is associated with a change in the spectral conditions of their habitat [Archer et al., 1995]. Myctophids show marked differences in habitat depending on their developmental stage, with larvae inhabiting the well-lit surface layers of the ocean [Sabates et al., 2003] and juvenile and adults occupying the deeper mesopelagic zone. Moreover, larvae and juvenile/adults also possess different types of photoreceptors, the larvae having both rods and cones [Bozzano et al., 2007], while juveniles/adults possess only rods. There is therefore a change in visual pigment expression between larval and juvenile/adult stage myctophids. However, microspectrophotometric results predict that both *Rh1* genes are expressed in the retina of the adult lanternfish, although it is unknown at this stage if both genes are also expressed in the larvae. While most deep-sea organisms produce bioluminescent emission in the blue-green region of the visible spectrum, several organisms do produce longer wavelength signals [Widder, 2010], the most extreme case being the red bioluminescence produced by some stomiid dragonfishes [Widder et al., 1984]. Some of these far-red illuminating fishes are known to prey on myctophids [Sutton and Hopkins, 1996], and the long-wave-shifted visual pigment in some of these lanternfishes (i.e. *M. nitidulum* and *M. obtusirostre*) could potentially have evolved as a mechanism to detect these predators [Hasegawa et al., 2008; Turner et al., 2009].

#### *Putative Functions of the Yellow Pigment in Myctophids*

Intra-ocular filters are thought to have many functions in vertebrates. In well-lit environments, they may improve visual acuity by reducing chromatic aberration and scatter (yellow lens and cornea [Walls, 1931; Walls and Judd, 1933; Muntz, 1973; Barbour et al., 2002]), enhance the discrimination of colours by narrowing the spectral sensitivity of the visual pigment (i.e. oil droplets [Hart, 2001]), filter out the potentially damaging short wavelengths present in bright environments [Collin et al., 2003] or allow the detection of fluorescent light emitted by certain organisms [Sparks et al., 2014]. In the deep sea, only 2 types of intra-ocular filters have been observed previously in teleosts: yellow lenses [Douglas and Thorpe, 1992] and the yellow pigmentation of the retina found in myctophids. In the mesopelagic zone, yellow lenses may increase hue discrimination in order to better visualise bioluminescent flashes or to break down the counterillu-

minating camouflage of other species [Muntz, 1976; Somiya, 1976, 1982; Douglas and Thorpe, 1992]. Indeed, during the day in the mesopelagic zone, the simultaneous presence of downwelling sunlight and bioluminescent flashes might render the detection of both signals difficult. More particularly, the presence of downwelling sunlight might reduce the contrast, and thereby the visibility, of bioluminescent emissions, which could be detrimental in terms of survival. However, since most bioluminescent emissions have a broader spectrum than downwelling light [Herring, 1983], yellow lenses might prevent this problem by cutting off most of the background illumination, thereby accentuating the signal. Lanternfish species with a yellow retinal pigmentation are found at very different depths during the day [de Busserolles et al., 2013]. However, at night they all migrate towards the surface to depths of <4 m [de Busserolles et al., 2013], where downwelling light produced by the moon and stars [Johnsen et al., 2004] may reduce the visibility of bioluminescent emissions. Therefore, in a similar way to yellow lenses, the presence of retinal yellow pigmentation could enhance the contrast of bioluminescent emissions against the night downwelling light in specific regions of the visual field.

Another potential function or outcome of yellow filtering in the mesopelagic realm is to increase the contrast of fluorescent objects such as siphonophores and other gelatinous zooplankton, which constitute regular prey [Kinzer and Schulz, 1985; Hopkins and Gartner, 1992; Beamish et al., 1999] and potential predators [Haddock et al., 2005; Pagès and Madin, 2010] of myctophids. Three areas of evidence support this idea. Firstly, several studies have shown that a number of mesopelagic animals both bioluminesce and fluoresce [Haddock et al., 2005, 2010; Widder, 2010]. Secondly, the light distribution in the mesopelagic zone, peaking around 475 nm (downwelling light and bioluminescence [Widder, 2010]), is well matched to the excitation wavelengths needed to trigger a variety of fluorescent marine compounds [Mazel et al., 2004; Haddock et al., 2005; Alieva et al., 2008; Vogt et al., 2008] and this means that, at the right depth and resulting light level, fluorescence may be a significant component of the signals from such animals. Thirdly, as the new wave of photographers interested in capturing fluorescence are aware [Mazel, 2005; www.nightsea.com], a yellow blocking filter enhances the contrast at longer wavelengths for yellow, orange or red emissions of fluorescence [Sparks et al., 2014]. This is because yellow removes the wash of blue excitation and leaves only the glowing fluorescent emission component, a highly contrasting signal, especially in

dim illumination. As a result, in addition to possibly enhancing the bioluminescent contrast, the yellow filters in the eyes of myctophids may also enable them to see fluorescent gelatinous prey and/or predators and any other fluorescent signals at depth.

Different species of lanternfishes possess different yellow-pigmented areas in the retina that may serve to enhance sensitivity to bioluminescence and/or fluorescence in different parts of the visual field. This implies inter-specific differences in behaviour. Myctophids show a variety of inter-specific differences in behaviour with respect to their depth distribution [Karnella, 1987], migration pattern [Watanabe et al., 1999] and diet [Kozlov, 1995; Shreeve et al., 2009; Van Noord et al., 2013]. Since all the species which possess a retinal yellow pigmentation vertically migrate to the surface at night, inter-specific differences in the location of the yellow pigmentation could potentially reflect differences in diet, a consequence of different nutritional requirements, niche partitioning and/or body size differences between males and females [Shine, 1989]. Unfortunately, data on diet are quite limited for lanternfishes and highly variable between seasons and geographic regions [Kozlov, 1995], making any diet/vision comparison impossible at this stage. Moreover, no studies have been conducted on possible diet differences between sexes, which would potentially explain the observed sexual dimorphism in the retinal yellow pigmentation. Sexual dimorphism in food choices has been reported in a number of organisms, as a consequence of different nutritional requirements, food competition, habitat and body size between males and females [Shine, 1989]. Sexual dimorphism in size has been observed in several lanternfish species [Gartner, 1993; Braga et al., 2008; Flynn and Paxton, 2012] and some differences in distribution between sexes have been suggested [Flynn and Paxton, 2012], supporting the possible role of the retinal yellow pigmentation in food choice.

The sexual dimorphism in the retinal yellow pigment implies a possible role in intra-specific/sexual communication. All of the species possessing the yellow pigment are also sexually dimorphic in the location and size of their caudal luminous organs, with all males possessing a large supracaudal organ and all females possessing a smaller infracaudal organ [Herring, 2007]. If the retinal yellow pigmentation is involved in sexual communication, inter-specific differences in the shape, size and location of the retinal pigment patches could be associated with differences in luminous organ location, size and shape between species, taking into consideration the po-

sition of the fish in the water column. Unfortunately, this information is not available for the species analysed and it is unknown how males and females position themselves with respect to one another in the water column. Further analyses of the retinal yellow pigmentation in both sexes, at several different life stages and from all the species possessing this yellow pigment will shed more light on the function and development of this new visual specialisation.

Overall, our findings indicate an evolutionary pressure to visualise prey/predators/mates in a specific part of each species' visual field. Our results also add a new dimension to the contribution made by recent studies [Davis et al., 2014; Kenaley et al., 2014] on the evolutionary history in the deep-sea by identifying a visual 'arms race', in term of visual adaptation, between lanternfishes and dragonfishes. In fact, while dragonfishes have evolved a secret communication/predation channel by using red bioluminescence, lanternfishes, by virtue of their visual sexual dimorphism, are taking the race a step further by inviting 'sex in the blue-light district of the deep sea'. It appears we have yet to unlock all of the secrets of bioluminescent communication in the deep sea.

### Acknowledgements

We wish to thank Dr. Mike Hall (AIMS) and the masters and crews of the RV *Cape Ferguson*, and Prof. Hans-Joachim Wagner (University of Tübingen, Germany) and the masters and crews of the FS *Sonne* for the sea time and sampling opportunities. We gratefully acknowledge John Denton and the American Museum of Natural History, New York, N.Y., USA, for providing the additional *M. brachygnathum* specimen, and John Paxton (Australian Museum) for providing most of the fish identification. We thank Prof. Julian Partridge (University of Bristol) for helpful discussions regarding the yellow pigment absorption spectra, and Eduardo Garza-Gisholt for his help using his R script for the creation of the yellow pigment maps. This work was supported by grants to S.P.C., N.S.H., D.M.H. and N.J.M. (DP110103294 and LP0775179) from the Australian Research Council and the West Australian State Government. W.I.D. is supported by the Australian Research Council (FT110100176 and DP140102117). F.d.B. was supported by a Scholarship for International Research Fees and a University International Stipend at the University of Western Australia.

## References

- Alieva NO, Konzen KA, Field SF, Meleshkevitch EA, Hunt ME, Beltran-Ramirez V, Miller DJ, Wiedenmann J, Salih A, Matz MV (2008): Diversity and evolution of coral fluorescent proteins. *PLoS One* 3:e2680.
- Appleby SJ, Muntz WRA (1979): Oclusable yellow corneas in Tetraodontidae. *J Exp Biol* 83: 249–259.
- Archer S, Hope A, Partridge JC (1995): The molecular basis for the green-blue sensitivity shift in the rod visual pigments of the European eel. *Proc Biol Sci* 262:289–295.
- Arikawa K, Wakakuwa M, Qiu X, Kurawasa M, Stavenga DG (2005): Sexual dimorphism of short-wavelength photoreceptors in the small white butterfly, *Pieris rapae crucivora*. *J Neurosci* 25:5935–5942.
- Baddeley A, Turner R (2005): Spatstat: an R package for analyzing spatial point patterns. *J Stat Softw* 12:1–42.
- Bailes HJ, Davies WL, Trezise AEO, Collin SP (2007): Visual pigments in a living fossil, the Australian lungfish *Neoceratodus forsteri*. *BMC Evol Biol* 7:200.
- Bailes HJ, Robinson SR, Trezise AEO, Collin SP (2006): Morphology, characterization, and distribution of retinal photoreceptors in the Australian lungfish *Neoceratodus forsteri* (Krefft, 1870). *J Comp Neurol* 494:381–397.
- Barbour HR, Archer MA, Hart NS, Thomas N, Dunlop SA, Beazley LD, Shand J (2002): Retinal characteristics of the ornate dragon lizard, *Ctenophorus ornatus*. *J Comp Neurol* 450: 334–344.
- Beamish RJ, Leask KD, Ivanov OA, Balanov AA, Orlov AM, Sinclair B (1999): The ecology, distribution, and abundance of midwater fishes of the Subarctic Pacific gyres. *Prog Oceanogr* 43:399–442.
- Bone RA, Landrum JT, Tarsis SL (1985): Preliminary identification of the human macular pigment. *Vision Res* 25:1531–1535.
- Bowmaker JK (2008): Evolution of vertebrate visual pigments. *Vision Res* 48:2022–2041.
- Bowmaker JK, Hunt DM (2006): Evolution of vertebrate visual pigments. *Curr Biol* 16:484–489.
- Bozzano A, Pankhurst PM, Sabatés A (2007): Early development of eye and retina in lanternfish larvae. *Vis Neurosci* 24:423–436.
- Braga AC, Costa PAS, Nunan GW (2008): First record of the firebrow lanternfish *Diaphus adenomus* (Myctophiformes: Myctophidae) from the South Atlantic. *J Fish Biol* 73:296–301.
- Cerda-Reverter JM, Haitina T, Schiøth HB, Peter RE (2005): Gene structure of the goldfish agouti-signaling protein: a putative role in the dorsal-ventral pigment pattern of fish. *Endocrinology* 146:1597–1610.
- Coimbra JP, Marceliano MLV, Andrade-da-Costa BLS, Yamada ES (2006): The retina of tyrant flycatchers: topographic organization of neuronal density and size in the ganglion cell layer of the great kiskadee *Pitangus sulphuratus* and the rusty margined flycatcher *Myiozetetes cayanensis* (Aves: Tyrannidae). *Brain Behav Evol* 68:15–25.
- Collin SP, Hart NS, Shand J, Potter IC (2003): Morphology and spectral absorption characteristics of retinal photoreceptors in the southern hemisphere lamprey (*Geotria australis*). *Vis Neurosci* 20:119–130.
- Crescitelli F (1990): Adaptations of visual pigments to the photic environment of the deep sea. *J Exp Zool* 256:66–75.
- Davies WL, Collin SP, Hunt DM (2012): Molecular ecology and adaptation of visual photopigments in craniates. *Mol Ecol* 21:3121–3158.
- Davies WL, Cowing JA, Bowmaker JK, Carvalho LS, Gower DJ, Hunt DM (2009): Shedding light on serpent sight: the visual pigments of henophidian snakes. *J Neurosci* 29:7519–7525.
- Davis MP, Holcroft NI, Wiley EO, Sparks JS, Smith WL (2014): Species-specific bioluminescence facilitates speciation in the deep sea. *Mar Biol* 161:1139–1148.
- de Busserolles F, Fitzpatrick JL, Marshall NJ, Collin SP (2014a): The influence of photoreceptor size and distribution on optical sensitivity in the eyes of lanternfishes (Myctophidae). *PLoS One* 9:e99957.
- de Busserolles F, Fitzpatrick JL, Paxton JR, Marshall NJ, Collin SP (2013): Eye-size variability in deep-sea lanternfishes (Myctophidae): an ecological and phylogenetic study. *PLoS One* 8:e58519.
- de Busserolles F, Marshall NJ, Collin SP (2014b): The eyes of lanternfishes (Myctophidae, teleostei): novel ocular specializations for vision in dim light. *J Comp Neurol* 522:1618–1640.
- Douglas RH, Hunt DM, Bowmaker JK (2003): Spectral sensitivity tuning in the deep-sea; in Collin SP, Marshall J (eds): *Sensory Processing in Aquatic Environments*. Berlin, Springer, pp 323–342.
- Douglas RH, Partridge JC (1997): On the visual pigments of deep-sea fish. *J Fish Biol* 50:68–85.
- Douglas RH, Thorpe A (1992): Short-wave absorbing pigments in the ocular lenses of deep-sea teleosts. *J Mar Biol Assoc UK* 72:93–112.
- Flynn AJ, Paxton JR (2012): Spawning aggregation of the lanternfish *Diaphus danae* (family Myctophidae) in the north-western Coral Sea and associations with tuna aggregations. *Mar Freshw Res* 63:1255–1271.
- Franceschini N, Hardie R, Ribí W, Kirschfeld K (1981): Sexual dimorphism in a photoreceptor. *Nature* 291:241–244.
- Gartner JV (1993): Patterns of reproduction in the dominant lanternfish species (Pisces: Myctophidae) of the eastern Gulf of Mexico, with a review of reproduction among tropical-subtropical Myctophidae. *Bull Mar Sci* 52: 721–750.
- Garza Gisholt E, Hemmi JM, Hart NS, Collin SP (2014): A comparison of spatial analysis methods for the construction of topographic maps of retinal cell density. *PLoS One* 9:e93485.
- Goldsmith TH, Collins JS, Licht S (1984): The cone oil droplets of avian retinas. *Vision Res* 24:1661–1671.
- Govardovskii VI, Fyhrquist N, Reuter T, Kuzmin DG, Donner K (2000): In search of the visual pigment template. *Vis Neurosci* 17:509–528.
- Haddock SHD, Dunn CW, Pugh PR, Schnitzler CE (2005): Bioluminescent and red-fluorescent lures in a deep-sea siphonophore. *Science* 309:263.
- Haddock SHD, Moline MA, Case JF (2010): Bioluminescence in the sea. *Ann Rev Mar Sci* 2: 443–493.
- Hart NS (2001): The visual ecology of avian photoreceptors. *Prog Retin Eye Res* 20:675–703.
- Hart NS (2002): Vision in the peafowl (Aves: *Pavo cristatus*). *J Exp Biol* 205:3925–3935.
- Hart NS, Coimbra JP, Collin SP, Westhoff G (2012): Photoreceptor types, visual pigments, and topographic specializations in the retinas of hydrophiid sea snakes. *J Comp Neurol* 520: 1246–1261.
- Hart NS, Lisney TJ, Marshall NJ, Collin SP (2004): Multiple cone visual pigments and the potential for trichromatic colour vision in two species of elasmobranch. *J Exp Biol* 207:4587–4594.
- Hart N, Partridge J, Cuthill I (1998): Visual pigments, oil droplets and cone photoreceptor distribution in the European starling (*Sturnus vulgaris*). *J Exp Biol* 201:1433–1446.
- Hart NS, Theiss SM, Harahush BK, Collin SP (2011): Microspectrophotometric evidence for cone monochromacy in sharks. *Naturwissenschaften* 98:193–201.
- Hasegawa EI, Sawada K, Abe K, Watanabe K, Uchikawa K, Okazaki K, Toyama M, Douglas RH (2008): The visual pigments of a deep-sea myctophid fish *Myctophum nitidulum* Garman: an HPLC and spectroscopic description of a non-paired rhodopsin-porphyrpsin system. *J Fish Biol* 72:937–945.
- Herring PJ (1983): The spectral characteristics of luminous marine organisms. *Proc R Soc Lond B Biol Sci* 220:183–217.
- Herring PJ (2007): Sex with the lights on? A review of bioluminescent sexual dimorphism in the sea. *J Mar Biol Assoc UK* 87:829–842.
- Hopkins TL, Gartner JV Jr (1992): Resource-partitioning and predation impact of a low-latitude myctophid community. *Mar Biol* 114: 185–197.
- Hornstein EP, O'Carroll DC, Anderson JC, Laughlin SB (2000): Sexual dimorphism matches photoreceptor performance to behavioural requirements. *Proc Biol Sci* 267: 2111–2117.
- Hunt DM, Dulai KS, Partridge JC, Cottrill P, Bowmaker JK (2001): The molecular basis for spectral tuning of rod visual pigments in deep-sea fish. *J Exp Biol* 204:3333–3344.
- Hunt DM, Fitzgibbon J, Slobodyanyuk SJ, Bowmakers JK (1996): Spectral tuning and molecular evolution of rod visual pigments in the species flock of cottoid fish in Lake Baikal. *Vision Res* 36:1217–1224.

- Hunt DM, Hart NS, Collin SP (2013): Sensory systems; in Trischitta F, Takei Y, Seibert P (eds): *Eel Physiology*. New York, CRC Press, pp 118–159.
- Hunt DM, Jacobs GH, Bowmaker JK (2005): The genetics of primate visual pigments; in Kremers J (ed): *The Primate Visual System: A Comparative Approach*. Chichester, Wiley.
- Ito S, Wakamatsu K (2003): Quantitative analysis of eumelanin and pheomelanin in humans, mice, and other animals: a comparative review. *Pigment Cell Res* 16:523–531.
- Johnsen S, Widder EA, Mobley CD (2004): Propagation and perception of bioluminescence: factors affecting counterillumination as a cryptic strategy. *Biol Bull* 207:1–16.
- Karnella C (1987): Family Myctophidae, lanternfishes; in Gibbs RH, Krueger WH (eds): *Biology of Midwater Fishes of the Bermuda Ocean Acre*. Washington, Smithsonian Institution Press, pp 51–168.
- Kenaley CP, DeVaney SC, Fjeran TT (2014): The complex evolutionary history of seeing red: molecular phylogeny and the evolution of an adaptive visual system in deep-sea dragonfishes (Stomiiformes: Stomiidae). *Evolution* 68:996–1013.
- Kinzer J, Schulz K (1985): Vertical distribution and feeding patterns of midwater fish in the central equatorial Atlantic. 1. Myctophidae. *Mar Biol* 85:313–322.
- Klovinis J, Schiöth HB (2005): Agouti-related proteins (AGRP) and agouti-signaling peptide (ASIP) in fish and chicken. *Ann NY Acad Sci* 1040:363–367.
- Kozlov AN (1995): A review of the trophic role of mesopelagic fish of the family Myctophidae in the Southern Ocean ecosystem. *CCAMLR Science* 2:71–77.
- Land MF (1984): Crustacea; in Ali MA (ed): *Photoreception and Vision in Invertebrates*. pp 401–438.
- Land MF (1988): The functions of eye and body movements in *Labidocera* and other copepods. *J Exp Biol* 140:381–391.
- Levine JS, MacNichol Jr EF (1985): Microspectrophotometry of primate photoreceptors: art, artefact and analysis; in Fein A, Levine JS (eds): *The Visual System*. New York, Liss, pp 73–87.
- Liu Y, Kempf VR, Brian Nofsinger J, Weinert EE, Rudnicki M, Wakamatsu K, Ito S, Simon JD (2003): Comparison of the structural and physical properties of human hair eumelanin following enzymatic or acid/base extraction. *Pigment Cell Res* 16:355–365.
- Lythgoe J, Partridge J (1989): Visual pigments and the acquisition of visual information. *J Exp Biol* 146:1–20.
- MacNichol Jr EF (1986): A unifying presentation of photopigment spectra. *Vision Res* 26:1543–1556.
- Mazel CH (2005): Underwater fluorescence photography in the presence of ambient light. *Limnol Oceanogr* 3:499–510.
- Mazel CH, Cronin TW, Caldwell RL, Marshall NJ (2004): Fluorescent enhancement of signaling in a mantis shrimp. *Science* 303:51.
- McGraw KJ (2006): Mechanics of uncommon colors: pterins, porphyrins and psittacofulvins; in Hill GE, McGraw KJ (eds): *Bird Coloration: Mechanism and Measurement*. Cambridge, Harvard University Press, pp 354–398.
- Meyer-Rochow VB, Lau TF (2008): Sexual dimorphism in the compound eye of the moth *Operophtera brumata* (Lepidoptera, Geometridae). *Invertebr Biol* 127:201–216.
- Morrow JM, Lazic S, Chang BSW (2011): A novel rhodopsin-like gene expressed in zebrafish retina. *Vis Neurosci* 28:325–335.
- Muntz W (1976): On yellow lenses in mesopelagic animals. *J Mar Biol Assoc UK* 56:963–976.
- Muntz WRA (1973): Yellow filters and the absorption of light by the visual pigments of some Amazonian fishes. *Vision Res* 13:2235–2254.
- Pagès F, Madin LP (2010): Siphonophores eat fish larger than their stomachs. *Deep Sea Res Part 2 Top Stud Oceanogr* 57:2248–2250.
- Parry JW, Bowmaker JK (2000): Visual pigment reconstitution in intact goldfish retina using synthetic retinaldehyde isomers. *Vision Res* 40:2241–2247.
- Partridge JC, Archer SN, Vanostrum J (1992): Single and multiple visual pigments in deep-sea fishes. *J Mar Biol Assoc UK* 72:113–130.
- Pointer MA, Carvalho LS, Cowing JA, Bowmaker JK, Hunt DM (2007): The visual pigments of a deep-sea teleost, the pearl eye *Scopelarchus analis*. *J Exp Biol* 210:2829–2835.
- Sabates A, Bozzano A, Vallvey I (2003): Feeding pattern and the visual light environment in myctophid fish larvae. *J Fish Biol* 63:1476–1490.
- Saitou N, Nei M (1987): The neighbor-joining method: a new method for reconstructing phylogenetic trees. *Mol Biol Evol* 4:406–425.
- Sedmak JJ, Weerasinghe D, Jolly S (1990): Extraction and quantitation of astaxanthin from *Phaffia rhodozyma*. *Biotechnol Tech* 4:107–112.
- Shine R (1989): Ecological causes for the evolution of sexual dimorphism: a review of the evidence. *Q Rev Biol* 64:419–461.
- Shreeve RS, Collins MA, Tarling GA, Main CE, Ward P, Johnston NM (2009): Feeding ecology of myctophid fishes in the northern Scotia Sea. *Mar Ecol Prog Ser* 386:221–236.
- Siebeck UE, Collin SP, Ghoddui M, Marshall NJ (2003): Oculable corneas in toadfishes: light transmission, movement and ultrastructure of pigment during light- and dark-adaptation. *J Exp Biol* 206:2177–2190.
- Sievers F, Wilm A, Dineen D, Gibson TJ, Karplus K, Li W, Lopez R, McWilliam H, Remmert M, Soding J, Thompson JD, Higgins DG (2011): Fast, scalable generation of high-quality protein multiple sequence alignments using Clustal Omega. *Mol Syst Biol* 7:539.
- Sison-Mangus MP, Bernard GD, Lampel J, Briscoe AD (2006): Beauty in the eye of the beholder: the two blue opsins of lycaenid butterflies and the opsin gene-driven evolution of sexually dimorphic eyes. *J Exp Biol* 209:3079–3090.
- Somiya H (1976): Functional significance of the yellow lens in the eyes of *Argyrops leucostictus*. *Mar Biol* 34:93–99.
- Somiya H (1982): ‘Yellow lens’ eyes of a stomioid deep-sea fish, *Malacosteus niger*. *Proc R Soc Lond B Biol Sci* 215:481–489.
- Sparks JS, Schelly RC, Smith WL, Davis MP, Tchernov D, Pieribone VA, Gruber DF (2014): The covert world of fish biofluorescence: a phylogenetically widespread and phenotypically variable phenomenon. *PLoS One* 9:e83259.
- Stone J (1981): *The Whole Mount Handbook: A Guide to the Preparation and Analysis of Retinal Whole Mounts*. Sydney, Maitland, p 128.
- Sutton TT, Hopkins TL (1996): Trophic ecology of the stomiid (Pisces: Stomiidae) fish assemblage of the eastern Gulf of Mexico: strategies, selectivity and impact of a top mesopelagic predator group. *Mar Biol* 127:179–192.
- Taft EB (1949): Melanin solubility in tissue sections. *Nature* 164:1133–1134.
- Tamura K, Stecher G, Peterson D, Kumar S (2013): MEGA6: Molecular Evolutionary Genetics Analysis version 6.0. *Mol Biol Evol* 30:2725–2729.
- Temple S, Hart NS, Marshall NJ, Collin SP (2010): A spitting image: specializations in archerfish eyes for vision at the interface between air and water. *Proc Biol Sci* 277:2607–2615.
- Thorpe A, Douglas RH, Truscott RJW (1993): Spectral transmission and short-wave absorbing pigments in the fish lens. 1. Phylogenetic distribution and identity. *Vision Res* 33:289–300.
- Thorpe A, Truscott RJW, Douglas RH (1992): Kynurenine identified as the short-wave absorbing lens pigment in the deep-sea fish *Stylephorus chordatus*. *Exp Eye Res* 55:53–57.
- Toomey MB, McGraw KJ (2007): Modified saponification and HPLC methods for analyzing carotenoids from the retina of quail: implications for its use as a nonprimate model species. *Invest Ophthalmol Vis Sci* 48:3976–3982.
- Toomey MB, McGraw KJ (2009): Seasonal, sexual, and quality related variation in retinal carotenoid accumulation in the house finch (*Carpodacus mexicanus*). *Funct Ecol* 23:321–329.
- Truscott RJW, Carver JA, Thorpe A, Douglas RH (1992): The identification of 3-hydroxykynurenine as the lens pigment in the gourami *Trichogaster trichopterus*. *Exp Eye Res* 54:1015–1017.
- Turner JR, White EM, Collins MA, Partridge JC, Douglas RH (2009): Vision in lanternfish (Myctophidae): adaptations for viewing bioluminescence in the deep-sea. *Deep Sea Res Part 1 Oceanogr Res Pap* 56:1003–1017.

- Ullmann JFP, Moore BA, Temple SE, Fernandez-Juricic E, Collin SP (2011): The retinal whole-mount technique: a window to understanding the brain and behaviour. *Brain Behav Evol* 79: 26–44.
- van Heyningen R (1971a): Fluorescent glucoside in the human lens. *Nature* 230:393–394.
- van Heyningen R (1971b): Fluorescent derivatives of 3-hydroxy-L-kynurenine in the lens of man, the baboon, and the grey squirrel. *Biochem J* 123:30–31.
- Van Noord JE, Olson RJ, Redfern JV, Kaufmann RS (2013): Diet and prey selectivity in three surface-migrating myctophids in the eastern tropical Pacific. *Ichthyol Res* 60:287–290.
- Vogt A, D'Angelo C, Oswald F, Denzel A, Mazel CH, Matz MV, Ivanchenko S, Nienhaus GU, Wiedenmann J (2008): A green fluorescent protein with photoswitchable emission from the deep sea. *PLoS One* 3:e3766.
- Walls GL (1931): The occurrence of colored lenses in the eyes of snakes and squirrels, and their probable significance. *Copeia* 1931:125–127.
- Walls GL, Judd H (1933): The intra-ocular colour-filters of vertebrates. *Br J Ophthalmol* 17: 641.
- Watanabe H, Moku M, Kawaguchi K, Ishimaru K, Ohno A (1999): Diel vertical migration of myctophid fishes (family Myctophidae) in the transitional waters of the western North Pacific. *Fish Oceanogr* 8:115–127.
- Widder EA, Latz MI, Herring PJ, Case JF (1984): Far red bioluminescence from two deep-sea fishes. *Science* 225:512–514.
- Widder EA (2002): Bioluminescence and the pelagic visual environment. *Mar Freshw Behav Physiol* 35:1–26.
- Widder EA (2010): Bioluminescence in the ocean: origins of biological, chemical, and ecological diversity. *Science* 328:704–708.
- Yokoyama R, Knox BE, Yokoyama S (1995): Rhodopsin from the fish, *Astyanax*: role of tyrosine 261 in the red shift. *Invest Ophthalmol Vis Sci* 36:939–945.
- Yokoyama S, Tada T, Zhang H, Britt L (2008): Elucidation of phenotypic adaptations: molecular analyses of dim-light vision proteins in vertebrates. *Proc Natl Acad Sci USA* 105: 13480–13485.
- Zeil J (1983): Sexual dimorphism in the visual system of flies: the compound eyes and neural superposition in bibionidae (Diptera). *J Comp Physiol A* 150:379–393.